

Short Contribution

Effect of Salinity on Estimating Geostrophic Transport of the Indonesian Throughflow along the IX1 XBT Section

YUN LIU¹, MING FENG^{2*}, JOHN CHURCH³ and DONGXIAO WANG¹

¹LED, South China Sea Institute of Oceanology, Chinese Academy of Sciences, Guangzhou, China

²CSIRO Marine Research, Floreat WA 6014, Australia

³CSIRO Marine Research, Hobart TAS 7001, Australia

(Received 30 April 2004; in revised form 28 October 2004; accepted 30 October 2004)

Geostrophic transport of the Indonesian Throughflow (ITF) is estimated from optimally-interpolated temperature data along a frequently repeated expendable bathythermograph (XBT) section between Fremantle, Australia and Sunda Strait, Indonesia and from two historical temperature-salinity (T/S) relationship products, CSIRO Atlas for Regional Seas (CARS) and Levitus (1982). The annual mean ITF geostrophic transport relative to 400 m during 1984–2001 is estimated to be 4.6 Sv using the CARS T/S relationship, which is about 20% higher than that found using the Levitus T/S relationship. This transport increment is due to the fact that the CARS T/S relationship, which incorporates more recent hydrographic data, better resolves the low-salinity signature of the ITF water. Isothermal averaging in the CARS T/S relationship may also improve representations of the water mass signatures in deep layers.

Keywords:

- Indonesian Throughflow,
- geostrophic transport,
- T/S relationship,
- XBT data,
- heat transport.

1. Introduction

The Indonesian throughflow (ITF) carries warm, low-salinity water, from the Pacific into the Indian Ocean through the Indonesian Seas. The ITF is the major connection between ocean basins at low latitudes and plays an important role in the heat transport of the global climate system (Gordon, 1986; Toole, 1987).

Measurement of the ITF volume transport has proved to be difficult due to the complex coastline and topography of the Indonesian Seas, as well as the highly variable nature of the currents in this region. Since 1983, a frequently repeated expendable bathythermograph (XBT) section has been operating between Fremantle, Australia and Sunda Strait, Indonesia (IX1 section) to measure upper ocean temperature and monitor the ITF variability (Fig. 1(a); Meyers *et al.*, 1995; Meyers, 1996; Meyers and Pigot, 1999; Wijffels and Meyers, 2004).

Using optimally-interpolated temperature during the first 6 years of XBT operation along IX1 and Levitus (1982, hereafter called Levitus82) temperature-salinity (T/S) relationship, Meyers *et al.* (1995) calculated the ITF

geostrophic transport relative to 400 m. The annual mean ITF transport was estimated to be 5 Sv ($1 \text{ Sv} = 10^6 \text{ m}^3\text{s}^{-1}$), with a peak of 12 Sv in August/September. Later, Meyers (1996) noted that the ITF transport during 1983–1994 had strong interannual variations that are related to the Pacific El Niño/Southern Oscillation (ENSO). Sprintall *et al.* (2002) updated this calculation and recognized the influence of mesoscale eddies on the ITF transport along IX1. They also pointed out the uncertainties of using historic salinity to calculate the ITF transport.

Levitus82 is a depth averaged climatology and is highly smoothed in space. New hydrographic data have been collected in this region in recent years, especially during late 1980's to mid 1990's (Bray *et al.*, 1997). A new T/S relationship (CSIRO Marine Research Atlas for Regional Seas, CARS) has been constructed by isothermal averaging and careful consideration of island barriers between the open ocean and Indonesian inner seas (Dunn and Ridgway, 2002).

In this study we use a bimonthly optimally-interpolated temperature product along IX1 (Meyers and Pigot, 1999) and the CARS and Levitus82 T/S relationships to quantify the salinity effect on the geostrophic transport estimate of the ITF, in order to set the scene for the usage of the CARS T/S relationship in the ITF research (S.

* Corresponding author. E-mail: Ming.Feng@csiro.au

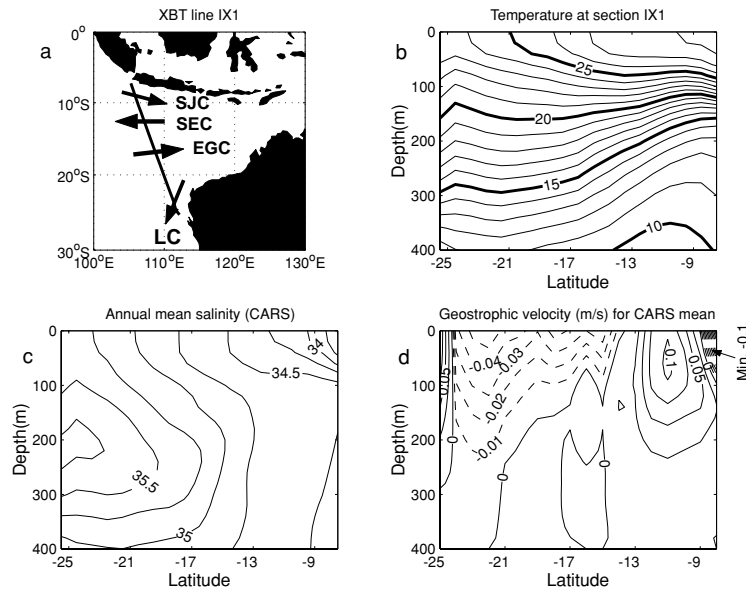


Fig. 1. (a) Location of the IX1 expendable bathythermograph (XBT) section, and (b) mean temperature, (c) salinity, and (d) geostrophic velocity structures using annual mean CARS T/S relationship along IX1. Westward velocity is positive.

Wijffels, 2003, personal communication). We focus on the salinity effect on the mean and annual cycle of the ITF transport. We are aware of interannual variations in the ITF salinity, which is addressed in a separate study (Phillips *et al.*, 2005).

2. Data

The optimally-interpolated temperatures along IX1 are on regular spatial grids and bimonthly temporal grids (January–February, February–March, etc.; Meyers and Pigot, 1999). In this study we use temperature data acquired during the period 1984–2001. Salinity along the section is derived from either the same Levitus82 T/S relationship as used by Meyers *et al.* (1995) or the new CARS T/S relationship. For better comparison with the results reported by Meyers *et al.*, we calculate dynamic height, geostrophic currents and volume transports referenced to 400 m. In the Discussion section, we also draw comparisons with results referenced to 700 m.

In Levitus82, temperature and salinity climatology were constructed separately as depth averages. There are much more upper ocean temperature casts than salinity measurements in the ITF region, so that the spatial smoothness of the two fields may not be compatible. Moreover, depth averaging could smear T/S structures near ocean fronts. The World Ocean Atlas 2001 (WOA01; Conkright *et al.*, 2002) adapted the same depth-averaging strategy, though it incorporates more recent hydrographic survey data in this region.

CARS is generated for the basic hydrographic fields using a locally weighted least square (LOESS) fit from

all available data in the regions surrounding Australia (Ridgway *et al.*, 2002; Dunn and Ridgway, 2002). The CARS T/S relationship is obtained by projecting salinity onto temperature surfaces before mapping onto regular grids. A special distance weighting function is used to avoid aliasing between different water masses segregated by land masses and islands. A sinusoidal function is used to represent the seasonal cycle in the T/S relationship. All the T/S relationships are linearly interpolated onto the XBT grid points.

3. Transport Difference Due to Different Annual Mean T/S Relationships

Major surface ocean currents along IX1 are denoted in Fig. 1(a), following Meyers (1996): the Leeuwin Current (LC) flows southwestward, within the Australian coastal waveguide; the eastward East gyral current (EGC) and westward South Equatorial Current (SEC) are in the middle of the section; and the South Java Current (SJC) is a shallow eastward current in the Sumatra-Java coastal waveguide. Major water masses along the section include the ITF low salinity water between about 10–14°S, the high salinity Indian Central Water off the Australian coast, and the very fresh SJC water (Figs. 1(c) and 2(a); Bray *et al.*, 1997). The currents are consistent with isothermal slopes, while the salinity distribution may also influence the current structure (Figs. 1(b) and (d)).

The SEC, which carries the bulk of the ITF water westward, extends from the reference depth (400 m) to the surface, with a peak westward velocity of about 0.1 m s⁻¹ at the subsurface (Fig. 1(d)). Part of the SEC water

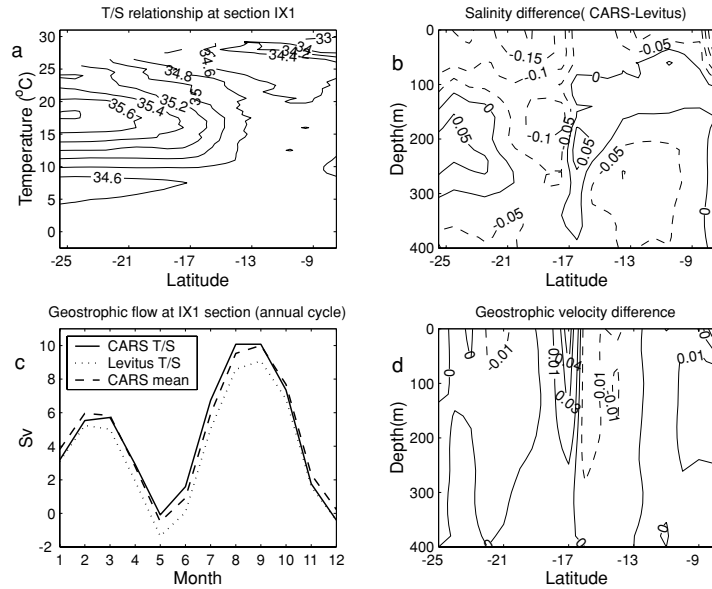


Fig. 2. (a) Annual mean CARS T/S relationship, (b) the mean salinity differences between annual mean CARS and Levitus82 T/S relationships, (c) annual cycle of total transports using different T/S relationships, and (d) mean geostrophic velocity differences (unit: m s^{-1}) between estimates using annual mean CARS and Levitus82 T/S relationships (westward is positive).

recirculates in the EGC (C. Domingues, 2003, personal communication). The EGC is shallow in the north, with near-zero geostrophic velocity below about 160 m. The southern portion of the EGC extends deeper, which partly feeds the LC. The largest mean eastward velocity occurs in the SJC off the Sumatra-Java coast.

The mean salinity from the CARS T/S relationship tends to be fresher than that found using the Levitus82 T/S relationship at sea surface (Fig. 2(b)). The CARS T/S relationship also better characterizes the subsurface low-salinity signature of the ITF water centered at 12°S and the high salinity signature of the Indian Central Water by about 0.05 psu. The SJC water is also fresher.

The annual and semiannual variations of the total ITF geostrophic transports across IX1 are similar using either the CARS (annual mean) or Levitus82 T/S relationships (Fig. 2(c)). The long-term mean (1984–2001) transport across IX1 using the CARS T/S relationship is 4.6 Sv, about 20% higher than that using the Levitus82 T/S relationship, 3.7 Sv. The number here is lower than that given in Meyers *et al.* (1995), which is due to interannual variations. Using the Levitus82 T/S relationship, our estimate of the mean ITF transport during 1984–1989 is 4.6 Sv, which is very close to Meyers *et al.* (1995).

Comparing the current structure and the vertically integrated transports using the CARS and Levitus82 T/S relationships, the largest differences occur between EGC and SEC (Figs. 2(d) and 3). The dividing position between the SEC and EGC using the CARS T/S relationship is located at 14.5°S , and the transition between the

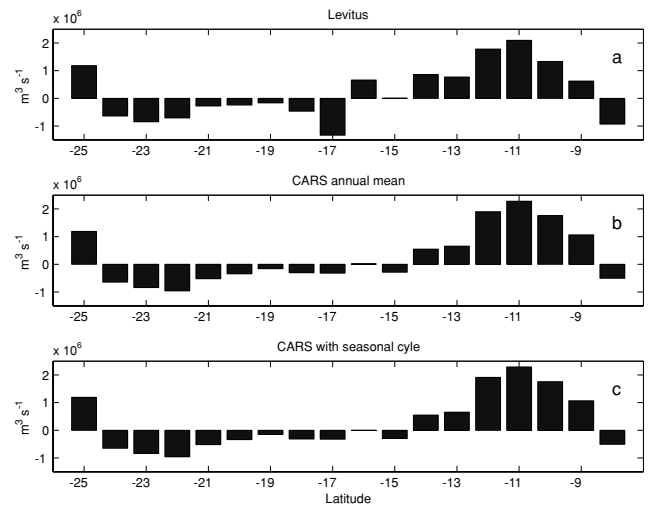


Fig. 3. Mean geostrophic transport for individual bin along IX1 using different T/S relationships.

two currents tends to be smoother than that using Levitus82 T/S relationship (which has a dividing position at 16.5°S). Note that two local maxima near 17°S in the subsurface salinity difference between CARS and Levitus82 (Fig. 1(c)), which causes the irregularity of the current there, are likely due to both the data coverage and the depth-averaging nature of the Levitus82 T/S relationship.

Table 1. Annual mean transports across the IX1 section*.

	LC	EGC	SEC	SJC	ITF
Latitude range	25.4–24.8°S	24.8–14.5°S	14.5–8.5°S	8.5–7.5°S	25.4–7.5°S
CARS T/S annual mean	1.19 (1.19 [†])	-4.34 (-4.67)	8.20 (7.96)	-0.50 (-0.50)	4.55 (3.98)
Levitus82 T/S	1.18 (1.18)	-4.00 (-4.29)	7.46 (7.43)	-0.93 (-0.93)	3.71 (3.39)
Difference [‡]	0.01 (0.01)	-0.34 (-0.38)	0.74 (0.53)	0.43 (0.43)	0.84 (0.59)
CARS T/S annual cycle	1.19	-4.38	8.23	-0.51	4.53

*Westward transport is positive and the unit is Sv.

[†]Numbers in parentheses are from f-plane approximations in the current segments.

[‡]Volume transport difference between using CARS annual mean and Levitus82 T/S relationships.

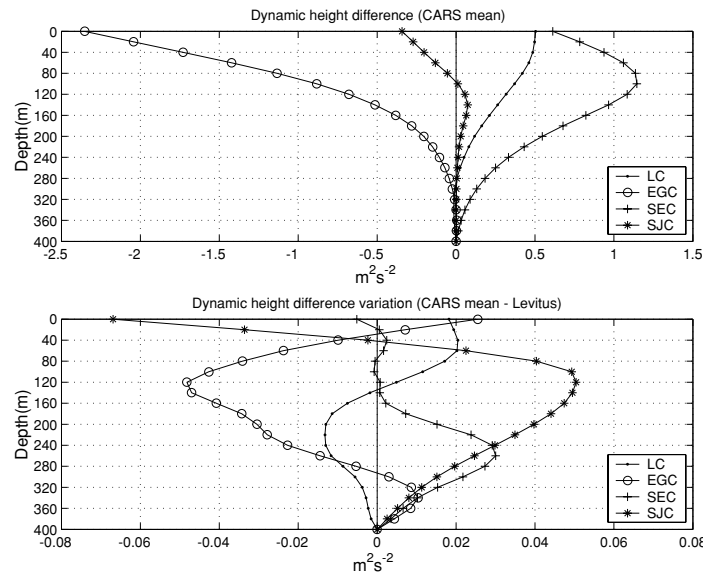


Fig. 4. (a) Mean dynamic height differences across the four current segments defined in Table 1 by using the annual mean CARS T/S relationship, and (b) variations in mean dynamic height differences between usages of the CARS and Levitus82 T/S relationships. Positive value denotes higher dynamic height in the south.

According to the transport distribution along IX1 from CARS T/S relationship, we divide the IX1 section into four segments to calculate the transports of the LC, EGC, SEC, and SJC respectively (Table 1). Using the annual mean CARS T/S relationship, the eastward transport of the SJC is reduced by 0.43 Sv compared to the Levitus82 T/S relationship, and there are increased transports in both the SEC and EGC, with larger increment in the SEC (Table 1). The transport variation in the LC is small.

Using an f-plane assumption, geostrophic transport is determined by the dynamic heights at its two end points at each segment (Fig. 4). The SJC is balanced by a shallow dynamic height difference (high at the coast) above 100 m, with a weak opposite gradient below to support a

westward mean undercurrent (Fig. 4(a)). Due to the lower salinity ITF water in the CARS T/S relationship, the dynamic height differences in the surface and subsurface are both enhanced (Fig. 4(b)). However, variation in the subsurface layers dominates over that in the surface layer, so that the net eastward transport in the SJC is reduced by nearly 50% (Table 1). At the southern boundary, the LC is balanced by a dynamic height difference (high at the coast) mostly in the upper 200 m (Fig. 4(a)). The effects of salinity differences on geostrophic volume transport cancel between the upper and lower layers (Fig. 4(b)), resulting little volume transport change (Table 1).

The difference between the oppositely flowing SEC and EGC contributes to nearly 90% of the net ITF transport (Table 1). The dynamic height difference across the

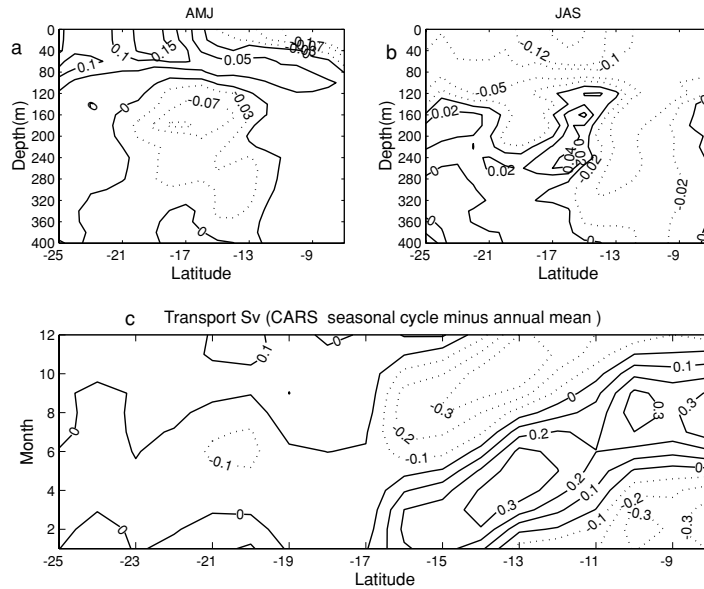


Fig. 5. Salinity deviations from annual mean during (a) April–June and (b) July–September in CARS T/S relationship, and (c) volume transport difference in the individual bins as in Fig. 3 between estimates using CARS T/S relationships with and without seasonal cycle.

SEC has a subsurface maximum, corresponding to its subsurface core (Fig. 4(a)). The use of the CARS T/S relationship increases the dynamic height differences across both currents (Fig. 4(b)). The increment across the SEC is confined at a depth between 200–400 m, and the increment across the EGC occurs between 40–290 m.

Although the increase in dynamic height difference across the EGC is larger than that across the SEC, the Coriolis coefficient at the center of the SEC (11.5°S) is $-2.9 \times 10^5 \text{ s}^{-1}$, about 60% of that at the center of EGC ($-4.9 \times 10^5 \text{ s}^{-1}$). The dynamic height difference changes across the two currents would account for slightly larger SEC transport changes than EGC in the two currents on *f*-planes (Table 1). Thus, a 0.21 Sv change in the SEC transport could not be explained by variation on an *f*-plane. The variation of the Coriolis coefficient within the SEC segment, that is, the β -effect, has to be taken into account. The salinity decreases in the ITF water between CARS and Levitus82 T/S relationships are located at the center of the SEC segment at both the surface and subsurface (Fig. 2(b)), which is able to contribute the increment of the SEC transport on a β -plane (Table 1). The EGC segment is located at higher latitudes so that the β -effect is weaker.

4. Effect of the T/S Relationship Seasonal Cycle

The annual salinity variation in the CARS T/S relationship has amplitudes of the order of 0.1 psu (Figs. 5(a) and (b)). In the southern portion of the section, surface

evaporation dominates over precipitation so that freshwater advection from the ITF is important to balance the salt budget. On the annual cycle, although there is greater freshwater loss during austral winter, the stronger ITF freshwater input overcomes the surface loss and causes negative salinity deviation during the winter time (Fig. 5(b)).

Including the seasonal cycle of CARS T/S relationship has little effects on the annual mean transport of both the total ITF and the individual currents at the IX1 section (Table 1, Fig. 3). However, the estimated ITF transport from CARS seasonal T/S relationship increases during the austral fall/winter (April–September) and decreases during the austral spring/summer, resulting a slightly stronger annual cycle than the result from annual mean T/S relationship (Fig. 2(c)). The transport difference is about 10% of the local transport in the north portion of section and it displays a northward phase propagation along IX1 (Fig. 5(c)). This propagation is likely to be a manifestation of a westward propagation (due to inclination of the XBT line, Fig. 1(a)) that is superimposed on an annual Rossby wave (Masumoto and Meyers, 1998).

5. Discussion and Summary

Using 700 m as the reference depth, there are larger discrepancies between the ITF volume transports estimated with the Levitus82 and CARS T/S relationships (Table 2). Nevertheless, there is little change in the annual mean transport with or without the annual cycle in

Table 2. Comparison of mean geostrophic current and heat transports of the ITF using 400 m and 700 m as reference depths.

Reference depth (m)	T/S relationship	Volume transport (Sv)	Heat transport (10^{14} W)	Time
400	CARS season	4.53	3.32	1986 Aug.–2001 Jul.
	Levitus82	3.74	2.83	
	CARS mean	4.54	3.34	
	WOA01 mean	4.74	3.54	
700	CARS season	6.30	4.88	1986 Aug.–2001 Jul.
	Levitus82	3.83	3.33	
	CARS mean	6.30	4.90	
	WOA01 mean	5.10	4.22	

the CARS T/S relationship. As suggested by one reviewer, we use a T/S relationship derived from the newly developed WOA01 climatology, which is constructed similarly to Levitus82 but has incorporated more recent data. There is less bias between the WOA01 and CARS salinities than that between Levitus82 and CARS, though the WOA01 climatology is still slightly saltier than the CARS climatology in the deep layers of the ITF (not shown). Using the WOA01 T/S relationship, the volume transport attains the same level as using CARS when referenced to 400 m. However, the usage of the WOA01 T/S relationship underestimates the ITF transport when referenced to 700 m. Thus, depth averaging may still cause biases of T/S relationship in deeper layers of WOA01 climatology.

Heat transport across the IX1 section is calculated relative to 0°C (Table 2). Levitus82 T/S relationship underestimates the ITF heat flux by 15 and 30% when the currents are referenced to 400 and 700 m respectively. Note that the difference would be higher if we use a higher reference temperature from observed data (S. Wijffels, personal communication). The heat flux estimates using the WOA01 also show improvements over that from Levitus82.

To summarize, the mean ITF transport reference to 400 m is 4.6 Sv during 1984–2001 using the CARS T/S relationship, which is about 20% higher than that using the Levitus82 T/S relationship. The increase of the ITF transport is due to the fact that the CARS T/S relationship better resolves the low-salinity signature of the ITF water. Both data coverage and isothermal averaging are important to capture T/S characteristics of the ITF water.

The ITF low-salinity advection dominates over the air-sea freshwater flux to govern the seasonal cycles of salinity along IX1. Using seasonally varying CARS T/S relationship, there tends to be enhanced ITF transport during the austral winter with weakened ITF transport during the austral summer, so that the estimated ITF transport has a stronger annual cycle.

Acknowledgements

This work was supported by a CSIRO-CAS exchange project, NSFC (Grant 40136010) and the CAS (Grant ZKCX2-SW-210). MF was also supported by the Strategic Research Fund for the Marine Environment. We would like to thank Gary Meyers and Lidia Pigot for providing the IXT XBT data, Jeff Dunn for providing CARS T/S relationships, and Susan Wijffels and two reviewers for critical comments.

References

- Bray, N. A., S. E. Wijffels, J. C. Chong, M. Fieux, S. Hautala, G. Meyers and W. M. L. Morawitz (1997): Characteristics of the Indo-Pacific throughflow in the eastern Indian Ocean. *Geophys. Res. Lett.*, **24**, 2569–2572.
- Conkright, M. E., R. A. Locarnini, H. E. Garcia, T. D. O'Brien, T. P. Boyer, C. Stephens and J. I. Antonov (2002): *World Ocean Atlas 2001: Objective Analyses, Data Statistics, and Figures, CD-ROM, Documentation*. National Oceanographic Data Center, Silver Spring, MD, 17 pp.
- Dunn, J. R. and K. R. Ridgway (2002): Mapping ocean properties in regions of complex topography. *Deep-Sea Res., Part I*, **49**, 591–604.
- Gordon, A. L. (1986): Inter-ocean exchange of thermocline water. *J. Geophys. Res.*, **91**, 5037–5046.
- Masumoto, Y. and G. Meyers (1998): Forced Rossby waves in the southern tropical Indian Ocean. *J. Geophys. Res.*, **103**, 27,589–27,602.
- Meyers, G. (1996): Variation of Indonesian throughflow and the El Niño–Southern Oscillation. *J. Geophys. Res.*, **101**, 12,255–12,263.
- Meyers, G. and L. Pigot (1999): Analysis of frequently repeated XBT lines in the Indian Ocean. Australia CSIRO Marine Laboratories Report, No. 238, 43 pp.
- Meyers, G., R. J. Bailey and A. P. Worby (1995): Geostrophic transport of Indonesian throughflow. *Deep-Sea Res., Part I*, **42**, 1163–1174.
- Phillips, H. E., S. E. Wijffels and M. Feng (2005): Interannual variability in the freshwater content of the Indonesian–Australian Basin. *Geophys. Res. Lett.*, **32**(3), L03603.
- Ridgway, K. R., J. R. Dunn and J. L. Wilkin (2002): Ocean

- interpolation by 4-dimensional weighted least squares—application to the waters around Australia. *J. Atmos. Ocean. Tech.*, **19**, 1357–1375.
- Sprintall, J., S. Wijffels, T. Chereskin and N. Bray (2002): The JADE and WOCE I10/IR6 Throughflow sections in the Southeast Indian Ocean. Part 2: Velocity and transports. *Deep-Sea Res., Part II*, **49**, 1363–1389.
- Toole, J. M. (1987): Problems of interbasins and marginal sea overflow. *Bull. Am. Meteor. Soc.*, **68**, 136–140.
- Wijffels, S. and G. Meyers (2004): An intersection of oceanic wave guides: variability in the Indonesian Throughflow. *J. Phys. Oceanogr.*, **34**, 1232–1253.